Article

Chinese Science Bulletin

Environmental Science & Technology

August 2011 Vol.56 No.24: 2644–2648
doi: 10.1007/s11434-011-4558-0

# Improved acetone sensing properties of flat sensors based on Co-$SnO_2$ composite nanofibers

HU Lei[1,2] & LI Yi[1,2*]

[1] *College of Environmental, Hohai University, Nanjing 210098, China;*
[2] *Key Laboratory of Integrated Regulation and Resource Development on Shallow Lakes of Ministry of Education, Hohai University, Nanjing 210098, China*

Received January 31, 2011; accepted April 22, 2011

Co-$SnO_2$ composite nanofibers were synthesized by an electrospinning method and characterized by X-ray diffraction, field emission scanning electron microscopy, and transmission electron microscopy. Gas sensors were fabricated by spinning these nanofibers onto flat ceramic substrates, which had signal electrodes and heaters on their top and bottom surfaces, respectively. Compared with sensors loaded with pure $SnO_2$ nanofibers, the Co-$SnO_2$ nanofiber sensors exhibited improved acetone sensing properties with high selectivity and rapid response and recovery times. The response was 33 when the sensors were exposed to 100 μL/L acetone at 330°C, and the corresponding response with 100 μL/L of ethanol was only 6. The response and recovery times to acetone were about 5 and 8 s, respectively. These results indicate Co-$SnO_2$ composite nanofibers are good candidates for fabrication of high performance acetone sensors for practical application.

**chemical sensors, gas sensors, semiconductor oxides, nanofibers, selectivity**

**Citation:** Hu L, Li Y. Improved acetone sensing properties of flat sensors based on Co-$SnO_2$ composite nanofibers. Chinese Sci Bull, 2011, 56: 2644–2648, doi: 10.1007/s11434-011-4558-0

Establishing effective methods for monitoring and detecting toxic and flammable gases such as carbon monoxide, acetone, benzene and toluene is important because of the regulations that exist in many countries [1–5]. Although many modern monitoring methods, such as gas chromatography and infrared spectroscopy, have high sensitivity, they are expensive and cannot be used for real-time measurements. Recently, semiconductor oxide-based gas sensors have attracted attention because of their good reproducibility, compact size, ease of use, and low cost [6,7]. However, the response time of these sensors is difficult to improve and their selectivity is low. The main reason for these problems is that the sensing reaction of these sensors is based on chemisorbed oxygen species on the sensor surface, and it is difficult to manipulate these oxygen species for specific outcomes [1]. The sensing performance is also based on the operating temperature, sensor structure, and material morphology. The interaction of these parameters is complex, and this makes it difficult to control or improve the semiconductor oxide-based gas sensors [8–10]. Recently, one-dimensional (1D) semiconductor oxides have received considerable attention because of their controllable diameter, high density of surface sites, and large surface-to-volume ratios. Many high performance gas sensors have been produced with rapid response/recovery times and high sensitivities [11–13]. Several Chinese groups have published a series of sensing results based on these 1D semiconductor oxides [12,13]. However, most of these sensors were fabricated by grinding the 1D semiconductor oxides into pastes and then coating the paste on the surface of ceramic tubes [7]. These processes would damage the morphology and structure of the oxides, and subsequently decrease the performance of the sensor. There have been few investigations on the selectivity of sensing with these sensors.

*Corresponding author (email: li_yi_2011@yahoo.cn)

Acetone is a commonly used chemical solvent that is toxic at high vapor concentrations. Even at concentrations well below those immediately dangerous to life and health (IDLH) it can have negative effects on human health [14–16]. Ethanol is another common chemical solvent, and is often present in the air when acetone sensing is conducted. However, the response characteristics of the semiconductor oxide sensors to acetone and ethanol are similar [14–16]. Consequently, improvement of the selectivity of the sensors for acetone and ethanol is important.

Here, a simple and effective route was developed for the fabrication of flat sensors with Co-$SnO_2$ composite nanofibers. To improve the sensitivity and response/recovery of the sensors, Co was doped into the $SnO_2$ nanofibers. The fabrication process employed for the flat sensors was selected to maintain the original morphology and structure of the nanofibers. This method may provide an alternative path for fabrication of high performance gas sensors for practical application [17].

## 1 Experimental

All chemicals (analytical grade reagents) were purchased from Tianjin Chemicals Co. Ltd. (Tianjin, China) and used as received without further purification. The electrospinning process was similar to that used in previous studies for metal oxide nanofiber synthesis [18–22]. Precursor solution was prepared from 1 g of polyvinylpyrrolidone ($M_t$=1300000) was dissolved in 5 g of ethanol and 5 g of *N*, *N*-dimethylformamide, followed by magnetic stirring for 1 h. This solution was then added into 0.5 g of $SnCl_2{\cdot}2H_2O$ and 0.02 g of $Co(NO_3)_2{\cdot}6H_2O$, and stirred vigorously for 6 h to yield a homogeneous mixture. The mixture was drawn into a hypodermic syringe at a constant flow rate of 1.2 mL/h, and then electrospun by applying 10 kV at an electrode distance of 20 cm. A piece of flat aluminum foil was used to collect the nanofibers. Pure $SnO_2$ nanofibers were synthesized by the same method without $Co(NO_3)_2{\cdot}6H_2O$.

Ceramic slides (Beijing Elite Tech Co., Ltd, Beijing, China) were used as the substrates, and masked for the electrode-spinning process. Six pairs of interlocking Ag-Pd electrodes (0.25 mm wide, 0.25 mm spacing) were placed on the aluminum foil in the electrospinning process (Figure 1(a)). The electrodes could be calcined at 800°C without any resistivity change. Platinum electrodes for controlling and measuring the sensor temperature were placed on the back of the substrates (Figure 1(b)). After spinning for about 2 h, the mask was removed, and the substrates were calcined at 600°C for 3 h.

Sensor measurement was performed using a chemical gas sensor (CGS-8, Beijing Elite Tech Co., Ltd, Beijing, China) intelligent gas sensing system (Figure 1(c)). The sensors were pre-heated at different operating temperatures for about 30 min. When the resistance of each sensor was stable,

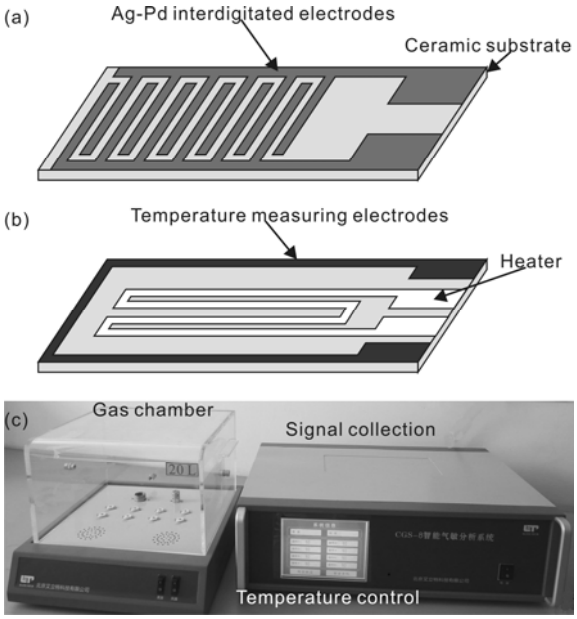


**Figure 1** Top (a) and bottom (b) views of the sensor substrate, and instrument setup for sensor measurement (c).

saturated target gas was injected into the test chamber (volume 20 L) by a micro-injector through a rubber plug. The saturated target gas was mixed with air (relative humidity 25%) by two fans in the analysis system. After the sensor resistance reached a constant value again, the test chamber was opened to recover the sensor in air. All the measurements were performed in a laboratory fume hood. The sensor resistance and sensitivity were acquired by the analysis system automatically.

The response value ($R$) was defined as $R=R_a/R_g$, where $R_a$ and $R_g$ are the sensor resistance in air and in a mixture of the target gas and air, respectively. The time taken by the sensor to achieve 90% of the total resistance change was defined as the response time for the response measurements (target gas adsorption) or the recovery time for the recovery measurements (target gas desorption).

X-ray diffraction (XRD) analysis was conducted on a Rigaku D/max-2500 X-ray diffractometer with Cu Kα radiation ($\lambda$=1.5418 Å). Field emission scanning electron microscopy (SEM) images were obtained on a JEOL JEM-6700F microscope operating at 5 kV. Transmission electron microscope (TEM) images were obtained on a JEOL JEM-2000EX microscope with an accelerating voltage of 200 kV.

## 2 Results and discussion

Figure 2 displays the XRD patterns of the pure and Co-doped $SnO_2$ nanofibers. Prominent peaks for the (110), (101) and (211) crystal lattice planes and all the other smaller peaks coincided with the corresponding peaks of the rutile

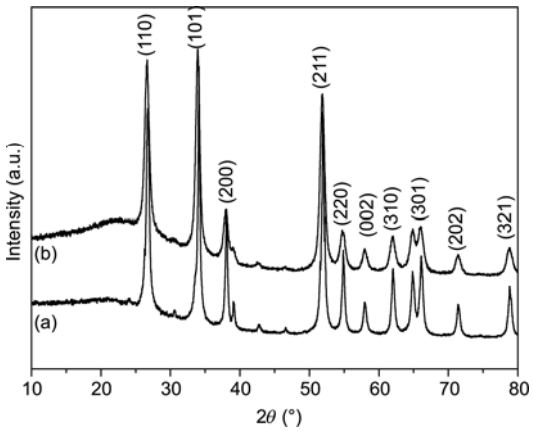


**Figure 2** XRD patterns of the pure and Co-doped $SnO_2$ nanofibers.

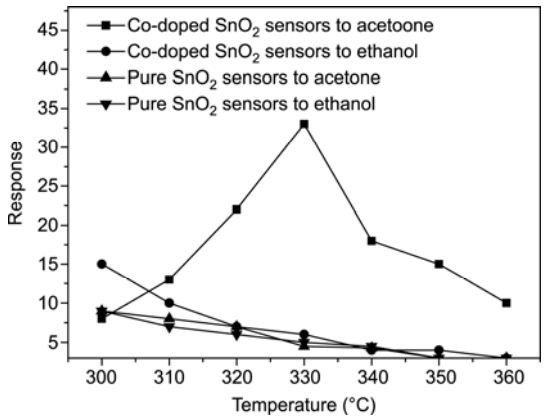


**Figure 4** Responses of the pure and Co-doped $SnO_2$ nanofiber-based flat sensors to 100 μL/L acetone and ethanol at different temperatures.

structure of $SnO_2$ (JCPDS File no. 41–1445) [23]. No diffraction peaks corresponding to CoO were observed in the Co-doped $SnO_2$ nanofibers, which indicates that Co may be doped into the $SnO_2$ nanofibers. No impurity peaks were observed.

Both pure and Co-doped $SnO_2$ nanofibers exhibited typical characteristics of nanofibers (Figure 3). The products were dominated by nanofibers with lengths of several tens of micrometers and diameters ranging from 60 to 130 nm. Features of the individual nanofibers were examined by TEM (Figure 3(a) and (b) inserts). The nanofibers consisted of many nanoparticles with an average diameter of about 20 nm. No obvious difference was found in the SEM and TEM images for the two samples, which indicates that the Co dopant does not change the fiber morphology markedly.

Figure 4 shows the relationship between the operating temperature and the response of the sensors to 100 μL/L acetone and ethanol, respectively. For the pure $SnO_2$ nanofiber-based flat sensors, the responses to acetone and ethanol were similar. While the Co-doped $SnO_2$ nanofiber-based flat sensors could successfully distinguish between these two target gases. The response of the Co-doped $SnO_2$ nanofiber-based flat sensor to 100 μL/L acetone was about 33 at 330°C, and was more than five times larger than that of the sensors to ethanol (response was about 6). These results suggest that the addition of Co is beneficial to the selective acetone sensing properties of $SnO_2$ nanofibers.

To further evaluate the selectivity of the Co-doped $SnO_2$ nanofiber-based flat sensor, sensors were exposed to different concentrations of acetone and ethanol at 330°C. As shown in Figure 5, the ability of the sensor to discriminate between these gases increased at higher concentrations. These results suggest that the selective detection of acetone can be achieved with this sensor, especially at high gas concentrations.

Figure 6 shows the responses of the Co-doped $SnO_2$

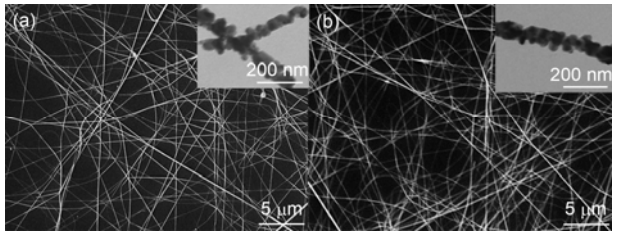


**Figure 3** SEM images of the pure (a) and Co-doped $SnO_2$ (b) nanofibers.

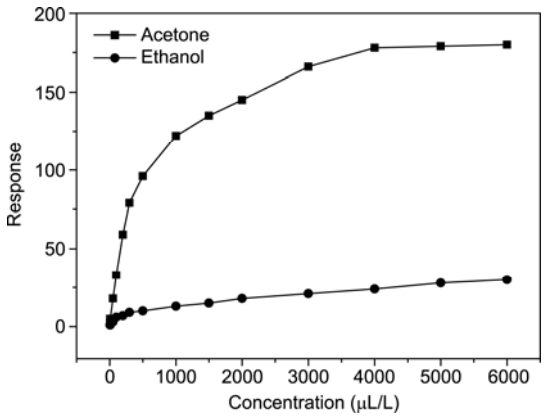


**Figure 5** Responses of the Co-doped $SnO_2$ nanofiber-based flat sensor to different concentrations of acetone and ethanol at 330°C.

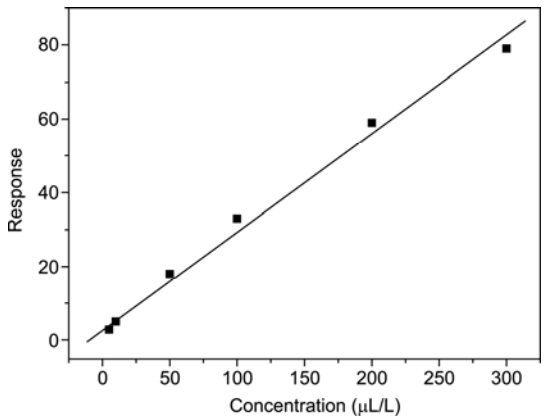


**Figure 6** Responses of the Co-doped $SnO_2$ nanofiber-based flat sensor to different concentrations (5–300 μL/L) of acetone at 330°C.

nanofiber-based flat sensor to different concentrations of acetone at 330°C. The relationship between sensor response and acetone concentration was linear between 5 and 300 μL/L, and the lowest detection limit was about 5 μL/L. These results further confirm that Co-doped $SnO_2$ nanofibers are promising for use in acetone sensors.

The change in sensor response with time to 100 μL/L acetone at 330°C is shown in Figure 7. The Co-doped $SnO_2$ nanofiber-based flat sensor exhibited very short response and recovery times. The signal become stable within 5 s (response time) after exposure to 100 μL/L acetone, and returned to the original value within 8 s (recovery time) after the target gas was replaced with air. These rapid response and recovery times are because of the 1D nanostructure, and this is discussed further later in the manuscript.

The sensor was also exposed to different gases (100 μL/L) at 330°C. The sensors also exhibited lower sensitive to $H_2$, $NH_3$, $CH_4$, liquefied petroleum gas, $C_6H_6$ and CO than to acetone (Figure 8). This indicates the developed sensor could be used in various practical applications because of its high selectivity.

The stability of the sensor was also investigated (Figure 9). The sensor exhibited nearly constant signals to 100, 500, and 1000 μL/L acetone during the tests, which confirms the good stability of the Co-doped $SnO_2$ nanofibers.

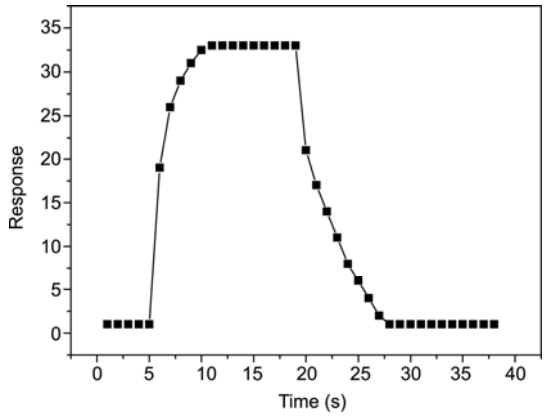


**Figure 7** Response versus time curve of Co-doped $SnO_2$ nanofiber-based flat sensors to 100 μL/L acetone at 330°C.

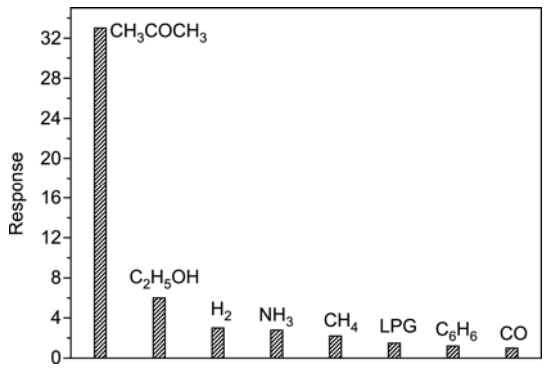


**Figure 8** Selectivity of the Co-doped $SnO_2$ nanofiber-based flat sensor with different gases (100 μL/L) at 330°C.

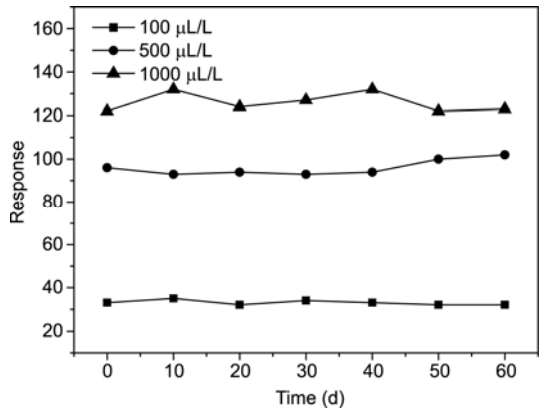


**Figure 9** Stability of Co-doped $SnO_2$ nanofiber-based flat sensors.

The sensing mechanism of $SnO_2$-based gas sensing materials has been discussed in many other papers [1,6–10]. Briefly, the change in resistance is primarily caused by the adsorption and desorption of the gas molecules on the surface of the sensing structure. When the $SnO_2$ nanofiber sensor is surrounded by air, oxygen molecules will adsorb on the fiber surface to generate chemisorbed oxygen species, of which $O^-$ is believed to be dominant. This leads to a decrease in the carrier concentration and electron mobility, which reduces the nanofibers conductivity. When the sensor is exposed to acetone, acetone molecules may react with the chemisorbed oxygen species and release the trapped electron back to the conduction band, which increases the carrier concentration and electron mobility and reduces the fiber's resistance. The 1D nanostructures of the $SnO_2$ nanofibers leads to the high response and short response/recovery times of the sensor [24–27]. The 1D nanostructures have high surface-to-volume ratios, and the high surface area provides many sites for adsorption of analyte molecules. The high surface-to-volume ratio also facilitate rapid mass transfer of the analyte molecules to and from the interaction region, and molecular recognition along the 1D nanostructure may create barriers that charge carriers need to transverse [11]. The fabrication process used in this study protects the fiber structure and morphology, which means that many netlike structures can form on the sensor surface. These netlike structures can make the sensor absorb more analyte molecules than other sensors, and this improves the sensor performance [28]. The acetone selectivity with Co doping is related to the change doping produced in the optimized operating temperature, which corresponds to the maximum response. $Co_3O_4$ is a p-type material, and when it is doped in n-type $SnO_2$, some p-n junctions may form in the sensing material. When the sensor is exposed to acetone, acetone molecules may permeate into the interface of the p-n junction, and lead to various changes in the sensor performance [29,30]. In this case (Figure 4), doping of Co into

the $SnO_2$ nanofibers increased the optimized operating temperature of the sensor for acetone to 330°C, but that for ethanol did not change. Therefore, Co may increase the total energy needed in the reaction between $SnO_2$ and acetone [31,32]. Other contributors to the acetone sensing characteristics include the uniform nanofiber structure and morphology, large surface to volume ratio, effective electron transport, and greatly reduced interfacial areas between the active sensing regions of the nanofibers.

## 3 Conclusions

Co-$SnO_2$ composite nanofibers were synthesized by an electrospinning method, and spun onto flat ceramic substrates with signal electrodes and heaters to produce sensors. These sensors exhibited improved acetone sensing properties compared to other sensors. They had a high response, rapid response and recovery times, improved selectivity, and good stability. These results indicate that Co-$SnO_2$ composite nanofibers could be used to fabricate practical acetone sensors with high performance.

*This work was supported by the Fundamental Research Funds for the Central Universities* (*B103046*)*, the Ministry of Education Key Laboratory of Integrated Regulation and Resource Development on Shallow Lakes Foundation, Hohai University* (*2008KJ003*)*, and Hohai University National Science Foundation* (*2008427211*)*.*

1 Narsan N, Koziej D, Weimar U. Metal oxide-based gas sensor research: How to? Sens Actuators B, 2007, 121: 18–35
2 Liu L, Zhuang J, Liu K X, et al. Improved and excellent ethanol sensing properties of $SnO_2$/multiwalled carbon nanotubes. Chinese Sci Bull, 2010, 55: 382–385
3 Tang H, Li Y, Zheng C, et al. An ethanol sensor based on cataluminescence on ZnO nanoparticles. Talanta, 2007, 72: 1593–1597
4 Deb B, Desai S, Sumanasekera G U, et al. Gas sensing behaviour of mat-like networked tungsten oxide nanowire thin films. Nanotechnology, 2007, 18: 285501
5 Tan E T H, Ho G W, Wong A S W, et al. Gas sensing properties of tin oxide nanostructures synthesized via a solid-state reaction method. Nanotechnology, 2008, 19: 255706
6 Liu L, Zhang T, Li S C, et al. Micro-structure sensor based on ZnO microcrystals with contact-controlled ethanol sensing. Chinese Sci Bull, 2009, 54: 4371–4375
7 Qi Q, Zhang T, Liu L, et al. Synthesis and toluene sensing properties of $SnO_2$ nanofibers. Sens Actuators B, 2009, 137: 471–475
8 Olbrechts B, Rue B, Suski J, et al. Characterization of FD SOI devices and VCO's on thin dielectric membranes under pressure. Solid-State Electron, 2007, 51: 1229–1237
9 Wang D, Chu X, Gong M. Hydrothermal growth of ZnO nanoscrewdrivers and their gas sensing properties. Nanotechnology, 2007, 18: 185601
10 Franke M E, Koplin T J, Simon U. Metal and metal oxide nanoparticles in chemiresistors: Does the nanoscale matter? Small, 2006, 3: 36–50
11 Kolmakov A, Moskovits M. Chemical sensing and catalysis by one-dimensional metal-oxide nanostructures. Annu Rev Mater Res, 2004, 34: 151–180
12 Chen Y, Zhu C, Wang T. The enhanced ethanol sensing properties of multi-walled carbon nanotubes/$SnO_2$ core/shell nanostructures. Nanotechnology, 2006, 17: 3012–3017
13 Li C C, Du Z F, Li L M, et al. Surface-depletion controlled gas sensing of ZnO nanorods grown at room temperature. Appl Phys Lett, 2007, 91: 032101
14 Gong H, Wang Y J, Teo S C, et al. Interaction between thin-film tin oxide gas sensor and five organic vapors. Sens Actuators B, 1999, 54: 232–235
15 Jing Z, Wu S. Synthesis, characterization and gas sensing properties of undoped and Co-doped $\gamma$-$Fe_2O_3$-based gas sensors. Mater Lett, 2006, 60: 952–956
16 Jie Z, Hua H L, Shan G, et al. Alcohols and acetone sensing properties of $SnO_2$ thin films deposited by dip-coating. Sens Actuators B, 2006, 115: 460–464
17 Huang J, Wan Q. Gas sensors based on semiconducting metal oxide one-dimensional nanostructures. Sensors, 2009, 9: 9903–9924
18 Li D, Xia Y. Electrospinning of nanofibers: Reinventing the wheel? Adv Mater, 2004, 16: 1151–1170
19 Kim I D, Rothschild A, Lee B H, et al. Ultrasensitive chemiresistors based on electrospun $TiO_2$ nanofibers. Nano Lett, 2006, 6: 2009–2013
20 Liu Z, Sun D D, Guo P, et al. An efficient bicomponent $TiO_2$/$SnO_2$ nanofiber photocatalyst fabricated by electrospinning with a side-by-side dual spinneret method. Nano Lett, 2007, 7: 1081–1085
21 Mccann J T, Li D, Xia Y. Electrospinning of nanofibers with core-sheath, hollow, or porous structures. J Mater Chem, 2005, 15: 735–738
22 Madhugiri S, Sun B, Smirniotis P G, et al. Electrospun mesoporous titanium dioxide fibers. Micropor Mesopor Mater, 2004, 69: 77–83
23 Sahm T, Mädler L, Gurlo A, et al. Flame spray synthesis of tin dioxide nanoparticles for gas sensing. Sens Actuators B, 2004, 98: 148–153
24 Huang X J, Choi Y K. Chemical sensors based on nanostructured materials. Sens Actuators B, 2007, 122: 659–671
25 Zhao H M, Chen Y, Quan X, et al. Preparation of Zn-doped $TiO_2$ nanotubes electrode and its application in pentachlorophenol photoelectro-catalytic degradation. Chinese Sci Bull, 2007, 52: 1456–1457
26 Ji H M, Lu H X, Ma D F, et al. Preparation and hydrogen gas sensitive characteristics of highly ordered titania nanotube arrays. Chinese Sci Bull, 2008, 53: 1352–1357
27 Wan Q, Li Q H, Chen Y J, et al. Fabrication and ethanol sensing characteristics of ZnO nanowire gas sensors. Appl Phys Lett, 2004, 84: 3654–3656
28 Zhang Y, He X, Li J, et al. Fabrication and ethanol-sensing properties of micro gas sensor based on electrospun $SnO_2$ nanofibers. Sens Actuators B, 2008, 132: 67–73
29 Kirby K W, Kimura H. Rapid evaluation processes for candidate CO and HC sensor materials: Examination of $SnO_2$, $CO_3O_4$, and $Cu_xMn_{3-x}O_4$ ($1<x\leqslant 1.5$). Sens Actuators B, 1996, 32: 49–56
30 Choi U S, Sakai G, Shimanoe K, et al. Sensing properties of $SnO_2$-$Co_3O_4$ composites to CO and $H_2$. Sens Actuators B, 2004, 98: 166–173
31 Patil L A, Patil D R. Heterocontact type CuO-modified $SnO_2$ sensor for the detection of a ppm level $H_2S$ gas at room temperature. Sens Actuators B, 2006, 120: 316–323
32 Choi J D, Choi G M. Electrical and CO gas sensing properties of layered ZnO-CuO sensor. Sens Actuators B, 2000, 69: 120–126